AUTOMATIC B-LINE DETECTION IN PAEDIATRIC LUNG ULTRASOUND

Nantheera Anantrasirichai[1], *Marco Allinovi*[2], *Wesley Hayes*[3], *Alin Achim*[1]

[1]Visual Information Lab, University of Bristol, Bristol, UK
[2]Paediatric Nephrology Unit, Meyer Childrens Hospital, Florence, Italy
[3]Great Ormond Street Hospital, London, UK

ABSTRACT

B-lines, defined as discrete laser-like vertical hyperechoic reverberation artefacts in lung ultrasounds, have been shown to correlate with extravascular lung water in symptomatic and asymptomatic adults and children on dialysis. Recent studies have shown this technique to be useful in children on dialysis. B-line detection in lung ultrasound in children is novel and challenging. This paper presents a novel automatic B-line detection via an inverse problem involving the Radon transform, which is solved using the alternating direction method of multipliers (ADMM). The proposed method restores the lines in the speckle images. Then, the B-lines are automatically detected using a simple local maxima technique in the Radon transform domain, associated with some definitions of the line artefacts. The results show that our proposed method outperforms existing methods by up to 69 %.

Index Terms— ultrasound, lung ultrasound, inverse problem, ADMM, line detection

1. INTRODUCTION

Fluid balance is an integral component of hemodialysis treatments to prevent under- or overhydration, both of which have been demonstrated to have significant effects on intradialytic morbidity and long-term cardiovascular complications. In recent years, the use of lung ultrasonography to detect extravascular lung water has received growing attention in clinical research in adult patients with heart failure, intensive care and chronic kidney disease undergoing hemodialysis (HD) and peritoneal dialysis (PD). Recent studies have shown the benefit of lung ultrasound in fluid assessment for children on dialysis [1, 2]. A key challenge in the detection of B-lines is operator dependency. Identifying and counting B-lines by eye are variable and open to error between different ultrasound operators.

During acquisition of lung ultrasonography, the difference in acoustic impedance between the lung and the surrounding tissues will be increased when lung density increases due to extravascular fluid. This results in some vertical narrow based lines arising from the pleural line to the edge of the ultrasound screen, known as B-lines. The presence of a few scattered B-line comets can be a normal variant, as found in healthy subjects, whilst multiple B-lines are considered the sonographic sign of lung interstitial syndrome [3].

Currently, the observation of B-lines in the lung ultrasonography is solely done by experts. However, to deal with the large data and to further analyse or use for detecting the early stage of some disease conditions, an automatic B-line detection is required. To the best of our knowledge, only two automatic approaches have been proposed in the literature [4, 5] and unfortunately their performances are still far from being reliable to use with the large data collected from different settings, particularly paediatric ultrasound data which differs from adult data given the anatomical differences between children and adults.

In this paper, we propose a novel solution to an inverse problem for line detection in the speckle ultrasound images. This aims to achieve B-line detection in children's lung ultrasound, which is more technically challenging due to chest size and rib positions. We employ a Radon transform, where a grayscale image is converted to a representation of radius and orientation as shown in Fig. 1. This inverse problem is solved using the alternating direction method of multipliers (ADMM) [6], offering fast convergence rate. We employ ℓ_1 regularisation since it gives good results for sparse data, such as lines in our work. We also propose an automatic robust method to detect B-lines, where the strong lines presented can simply be detected from local peaks in the Radon transformed domain.

The remainder of this paper is organised as follows. The background and related work in this field is stated in Section 2. The proposed line detection method is described in Section 3. The performance of the method is evaluated in Section 4. Finally, Section 5 presents the conclusions of this work.

2. BACKGROUND

When lung density increases due to the presence in the lung of transudate, the acoustic mismatch between the lung and the surrounding tissues is lowered, and the ultrasound beam can be partly reflected at deeper zones and repeatedly. This phenomenon creates some vertical reverberation artefacts known

as B-lines [7]. Similarly appearing artefacts that should not be confused with B-lines are Z-lines. They are short, broad, ill defined, vertical comet tail artefacts arising from the pleural line but not reaching the distal edge of the screen. They are less echogenic than the pleural line and do not erase A-lines. The A-lines are repetitive horizontal echoic lines with equidistant intervals, which are also equal to the distance between skin and pleural line.

Two automatic B-line detection techniques have been proposed in the literature. The first method was proposed by Brattain et al. [4] using angular features and thresholding (AFT). Five features are employed and the B-line is detected in a particular image column if each feature exceeds a predefined threshold. This method is not robust to the different machine settings, as noise and intensity of the images can be significantly different thereby requiring different values of the threshold. The second method was proposed by Moshavegh et al. [5] using alternate sequential filtering (ASF). Firstly, the method detects the pleural line using a random walk technique. The binary mask for the area underneath the pleural line is then generated from the absolute values of the Hilbert transform of the axial gradient components. A repeated sequential morphological opening and closing approach is applied to the mask until possible B-lines are separated. The drawback of this method is that the results always overestimate the number of B-lines because the Z-lines are not discarded. A semi-automatic approach was proposed by Weitzel et al. [8]. The users define the area below the pleural line. The moving average filter is employed and a pre-defined thresholding technique is used to identify the B-line.

3. PROPOSED METHOD

This section describes the proposed method of line restoration via an inverse problem, presented in Section 3.1, and the proposed automatic B-line detection method, presented in Section 3.2.

3.1. Line Detection in speckle images

Lines in the noisy ultrasound image are described using the model

$$y = \mathcal{R}^{-1}x + n, \tag{1}$$

where y is the observed ultrasound image, x is the line represented by the orientation θ and distance ρ from the centre of y. $\mathcal{R}$ and $\mathcal{R}^{-1}$ are a Radon transform and an inverse Radon transform, respectively. n is Gaussian noise.

In a formulation without a noise term, a Radon transform is described as in Eq. 2, where $\delta(\bullet)$ is the delta function. To operate with an image, the $\mathcal{R}$ and $\mathcal{R}^{-1}$ are discrete versions, which can be implemented as proposed in [9].

$$x = \int_{\mathbb{R}^2} y(i,j)\delta(\rho - i\cos\theta - j\sin\theta)didj. \tag{2}$$

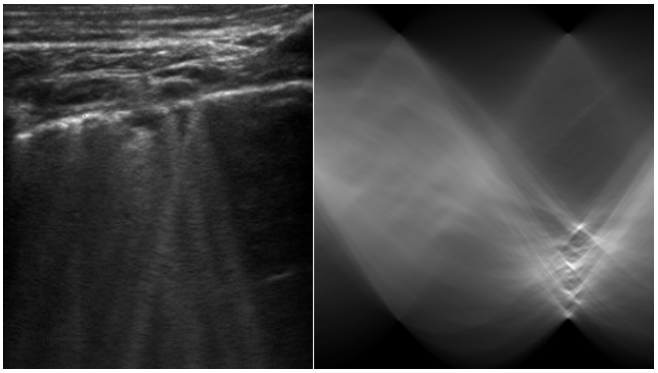

Fig. 1. Example of lung ultrasound image y (left column) and its Radon transform $\mathcal{R}y$ (right column), where the horizontal axis is θ varying from -45° to 135°, the vertical axis is ρ varying from $-\rho_{max}$ to ρ_{max}, and the brighter intensity indicates higher magnitude of the Radon transform.

Lines x can be estimated using ℓ_1 regularisation approach as

$$x = \arg\min_x \{\frac{1}{2}||y - \mathcal{R}^{-1}x||_2^2 + \alpha||x|| + \beta||\nabla\mathcal{R}^{-1}x||\}, \tag{3}$$

where α and β are regularisation constants. The first two terms are similar to the method proposed in [10]. The third term is included in the estimation because the output of the Radon transform is quantised by a discrete pre-defined range of orientation Θ. ∇g is the gradient of g, defined as $\nabla g = (g_{xx}g_y^2 - 2g_x g_y g_{xy} + g_{yy}g_x^2)/(g_x^2 + g_y^2)$, where g_x and g_y are $\frac{\partial g}{\partial x}$ and $\frac{\partial g}{\partial y}$ in horizontal and vertical directions, respectively. This regularisation term is similar to that in a super-resolution approach for compressed video [11], which is used to suppress quantisation noise.

3.1.1. Alternating direction method of multipliers

The alternating direction method of multipliers (ADMM) [6] is employed to solve the problem in Eq. 3. It is a variant of the augmented Lagrangian scheme that uses partial updates for the dual variables. It is simple to implement by splitting a large problem into a series of subproblems as follows.

$$\begin{aligned} &\text{minimize} \;\; f(u) + g(x), \\ &\text{subject to} \;\; u - x = 0. \end{aligned} \tag{4}$$

where

$$f(u) = \frac{1}{2}||y - \mathcal{R}^{-1}u||_2^2, \tag{5a}$$

$$g(x) = \alpha||x|| + \beta||\nabla\mathcal{R}^{-1}x||. \tag{5b}$$

Then, the Augmented Lagrangian for (4) is

$$\begin{aligned} \mathcal{L}_\rho(u,x,z) =& \frac{1}{2}||y - \mathcal{R}^{-1}u||_2^2 + \beta||\nabla\mathcal{R}^{-1}x|| \\ &+ \alpha||x|| + z^T(u-x) + \frac{\gamma}{2}||u-x||_2^2, \end{aligned} \tag{6}$$

where z is the dual variable or Lagrange multiplier. $\gamma > 0$ is a penalty parameter and z^T indicates the transport of z.

The ADMM technique allows this problem to be solved approximately by first solving for u with x fixed, and then solving for x with u fixed. The computation process consists of three-step iterations, namely i) u-minimisation, ii) x-minimisation, and iii) dual update, as follows.

$$u^{k+1} := \arg\min_u \mathcal{L}_\gamma(u, x^k, z^k), \tag{7a}$$

$$x^{k+1} := \arg\min_x \mathcal{L}_\gamma(u^{k+1}, x, z^k), \tag{7b}$$

$$z^{k+1} := z^k + \gamma(u^{k+1} - x^{k+1}). \tag{7c}$$

where k is an internal iteration counter.

3.1.2. Implementation

The problem in (7a) is a quadratic function about u, which can be solved as in Eq. 8, where $\mathcal{I}$ is the identity matrix.

$$\begin{aligned} u^{k+1} &= \arg\min_u \frac{1}{2}||y - \mathcal{R}^{-1}u||_2^2 + (z^k)^T(u - x^k) \\ &\quad + \frac{\gamma}{2}||u - x^k||_2^2, \\ &= ((\mathcal{R}^{-1})^T\mathcal{R}^{-1} + \gamma\mathcal{I})^{-1}((\mathcal{R}^{-1})^T y + \gamma x^k - z^k). \end{aligned} \tag{8}$$

To solve Eq. (7b), we first ignore $\beta||\nabla\mathcal{R}^{-1}x||$ for simplicity, then we have

$$\begin{aligned} x^{k+1} &= \arg\min_x \frac{\alpha}{\gamma}||x|| + \frac{1}{2}||u^{k+1} - x + \frac{z^k}{\gamma}||_2^2, \\ &= S_{\alpha/\gamma}\left(u^{k+1} + \frac{z^k}{\gamma}\right). \end{aligned} \tag{9}$$

where $S_\lambda(\bullet)$ is a soft thresholding described as

$$S_\lambda(a) = sign(a)\max(|a| - \lambda, 0). \tag{10}$$

Subsequently, we apply a smooth function to suppress the quantisation noise, occurring due to a discrete pre-defined range of orientation Θ. Denoting $\tilde{y}^{k+1}$ as the line image of x^{k+1}, $\tilde{y}^{k+1} = \mathcal{R}^{-1}x^{k+1}$. Then, x^{k+1} is updated as described in Eq. 11.

$$x^{k+1} = \mathcal{R}\left(\tilde{y}^{k+1} + \beta\nabla\tilde{y}^{k+1}\right) \tag{11}$$

Note that if the step size for θ is very small, e.g. $\Delta\theta < 0.25°$, this smooth term can be removed.

The last step in each iteration is for updating z, which is

$$z^{k+1} = z^k + \gamma(u^{k+1} - x^{k+1}). \tag{12}$$

3.2. B-line Detection

The exact number of B-lines must be sought on the pleural line, i.e. it is equivalent to the number of points from which lines originate. Therefore, the procedure starts with detecting the pleural line in the restored x, using the fact that it is always the brightest line. The search area of the maximum value is limited to $\Theta_p \in [70°, 110°]$ ($0°$ starts from the x axis), and limiting the range of ρ to $\rho > 0$ since the pleural line is always located on the top half of the image. Then the A-lines, physiological horizontal lines below the pleural line, are detected using $\Theta_A = \Theta_p$ and the fact that they are equidistant. The lines are detected using local maxima technique proposed in [12]. The B-lines are detected at $\Theta_B \in [-20°, 20°]$. The A-lines are erased by the B-lines, so any vertical artefacts with the presence of the A-lines are removed – these artefacts are called Z-lines which are not used for diagnosis. Any detected vertical lines that merge at the pleural line are counted as a single B-line.

4. RESULTS AND DISCUSSION

We tested our methods with 50 paediatric lung ultrasound images. They were acquired using linear array transducers because they were best suited to small body size. If convex transducers are used, the images have to be transformed to rectangular images, which can be done using affine transform. We set α, β and γ equal to 1 throughout the experiment. The algorithm stopped with the convergence criterion $||x^{k+1} - x^k||/||x^k|| < 10^{-3}$, resulting in the process ending in <25 iterations.

The subjective results in Fig. 2 show the detected pleural, A-, B- and Z-lines (red = pleural line, blue = A-lines, yellow = B-lines, green = Z-lines). Fig. 3 shows the comparison of our method with two existing approaches for automatic B-line detection, which are i) angular features and thresholding (AFT) [4] and ii) alternate sequential filtering (ASF) [5]. The x-axis is the number of B-lines identified by the expert and y-axis is the results marked by automated approaches. Our method achieves the best mean square error (MSE) which is 0.45, whilst the MSE of the AFT and ASF are 1.44 and 1.02, respectively. Both existing techniques overestimate the number of B-lines when it should be 0 or 1, since A-lines are not taken into account, resulting in Z-lines being misclassified. They underestimate when the number of B-lines is between 2-4, since the shadow of the ribs in children causes unclear/fade laser-like artefacts, unlike those in the adult cases.

5. CONCLUSION

This paper presents two novel algorithms for automated detection of B-lines in lung ultrasound images. The first method restores the lines in the speckle images by solving an inverse problem based on the Radon transform. The proposed method offers a simple and fast implementation via alternating direction method of multipliers. With the accurate line detection results from the first method, the second method identifies B-lines automatically from the local maxima in the Radon trans-

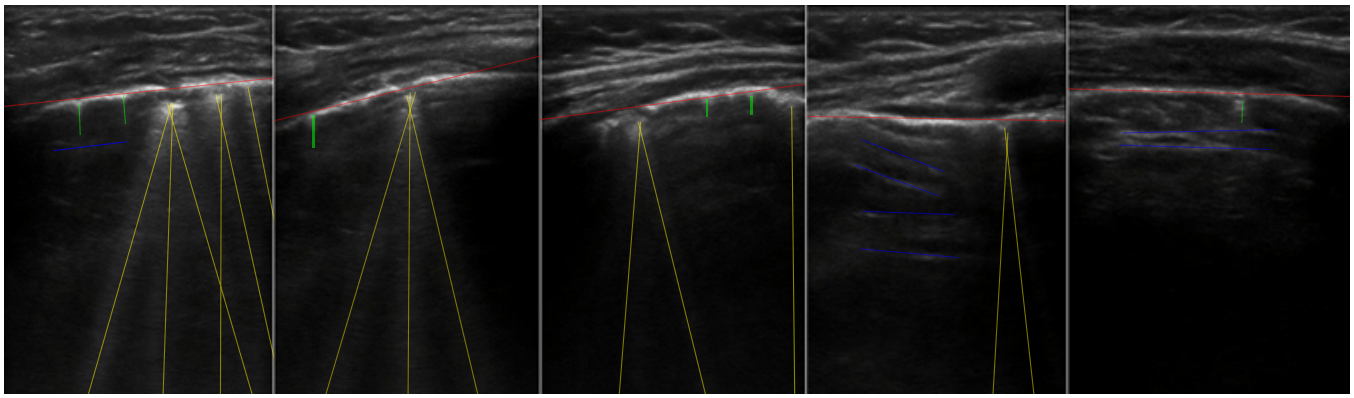

(a) (b) (c) (d) (e)

Fig. 2. Lung ultrasound images with (a) three B-lines and two Z-lines, (b) one B-line and one Z-line, (c) two B-lines and three Z-lines, (d) one B-line and several A-lines, and (e) Z-line and several A-lines. Note that the pleural line is red, the B-lines are yellow, the Z-lines are green, and the A-lines are blue.

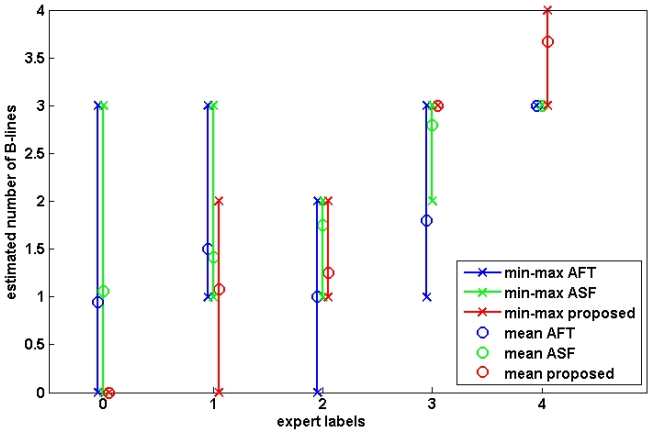

Fig. 3. Estimation of the number of B lines. MSE of AFT, ASF and the proposed method are 1.44, 1.02 and 0.45, respectively

form domain. The results show that our proposed method outperforms two existing automatic B-line detection up to 69 %. Future work will combine despeckling [13, 14] and PSF estimation as inverse problems for the case when the input is a raw radiofrequency image.

6. REFERENCES

[1] M. Allinovi, M.A. Saleem, O. Burgess, C. Armstrong, and W. Hayes, "Lung ultrasound: a novel technique for detecting fluid overload in children on dialysis," *Nephrol. Dial. Transplant.*, 2016.

[2] M. Allinovi, M.A. Saleem, O. Burgess, C. Armstrong, and W. Hayes, "Finding covert fluid: methods for detecting volume overload in children on dialysis," *Pediatr Nephrol.*, 2016.

[3] G. Soldati, R. Copetti, and S. Sher, "Sonographic interstitial syndrome: The sound of lung water," *J. Ultrasound Med.*, vol. 28, pp. 163–174, 2009.

[4] L. J. Brattain, B. A. Telfer, A. S. Liteplo, and V. E. Noble, "Automated B-line scoring on thoracic sonography," *J. Ultrasound Med.*, vol. 32, no. 12, pp. 2185–2190, Dec. 2013.

[5] R. Moshavegh, K. L. Hansen, H. Møller Sørensen, M. C. Hemmsen, C. Ewertsen, M. B. Nielsen, and J. A. Jensen, "Novel automatic detection of pleura and B-lines (comet-tail artifacts) on in vivo lung ultrasound scans," in *SPIE Medical Imaging: Ultrasonic Imaging and Tomography*, 2016, pp. 1–7.

[6] S. Boyd, N. Parikh, E. Chu, B. Peleato, and J. Eckstein, "Distributed optimization and statistical learning via the alternating direction method of multipliers," *Foundations and Trends in Machine Learning*, vol. 3, no. 1, pp. 1–122, 2011.

[7] D. A. Lichtenstein, G. A. Mezière, J.-F. Lagoueyte, P. Biderman, I. Goldstein, and A. Gepner, "A-lines and b-lines: Lung ultrasound as a bedside tool for predicting pulmonary artery occlusion pressure in the critically ill," *Chest*, vol. 136, no. 4, pp. 1014–1020, 2009.

[8] W.F.Weitzel, J.Hamilton, X.Wang, J.L.Bull, A.Vollmer, A.Bowman, J.Rubin, G.H.Kruger, J.Gao, M.Heung, and P.Rao, "Quantitative lung ultrasound comet measurement: Method and initial clinicalresults," *Blood Purif*, vol. 39, pp. 37–44, 2015.

[9] B. T. Kelley and V. K. Madisetti, "The fast discrete Radon transform: I. Theory," *IEEE Transactions on Image Processing*, vol. 2, no. 3, pp. 382–400, Jul 1993.

[10] N. Aggarwal and W. C. Karl, "Line detection in images through regularized Hough transform," *IEEE Transactions on Image Processing*, vol. 15, no. 3, pp. 582–591, March 2006.

[11] N. Anantrasirichai and C. N. Canagarajah, "Spatiotemporal super-resolution for low bitrate H.264 video," in *IEEE International Conference on Image Processing*, 2010, pp. 2809–2812.

[12] D. G. Lowe, "Distinctive image features from scale-invariant keypoints," *International Journal of Computer Vision*, vol. 60, no. 2, pp. 91–110, 2004.

[13] A. Achim, A. Bezerianos, and P. Tsakalides, "Novel bayesian multiscale method for speckle removal in medical ultrasound images," *IEEE Transactions on Medical Imaging*, vol. 20, no. 8, pp. 772–783, Aug. 2001.

[14] N. Anantrasirichai, L. Nicholson, J. E. Morgan, I. Erchova, K. Mortlock, R. V. North, J. Albon, and A. Achim, "Adaptive-weighted bilateral filtering and other pre-processing techniques for optical coherence tomography," *Computerized Medical Imaging and Graphics*, vol. 38, no. 6, pp. 526–539, Sep. 2014.